

# PHYTOFABRICATION OF SILVER NANO PARTICLES USING *OCIMUM SANCTUM* LEAF EXTRACT AND THEIR ANTIBACTERIAL AND ANTICANCER ACTIVITY THROUGH OXIDATIVE DAMAGE

Debbethi Bera <sup>a,b</sup>, Kunal Pal <sup>c,d</sup>, Parimal Karmakar <sup>c</sup>, Sukhen Das <sup>b</sup>, Papiya Nandy <sup>a\*</sup>

<sup>a</sup> Department of Physics, Jadavpur University  
Kolkata-700032, India

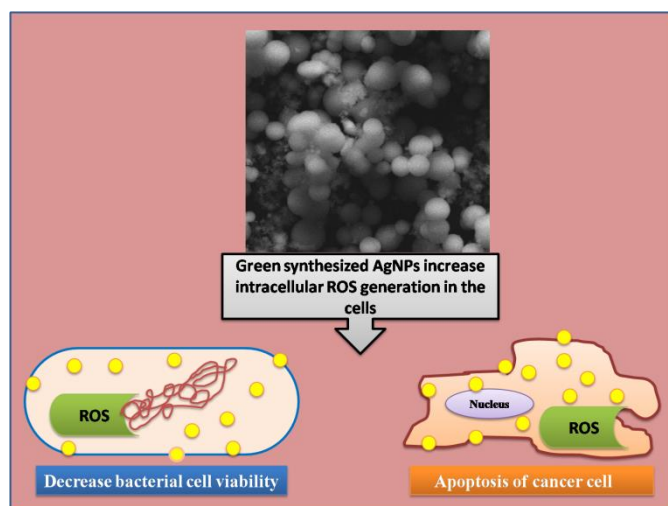
<sup>b</sup> Centre for Interdisciplinary Research and Education  
404B, Jodhpur Park, Kolkata-700068, India

<sup>c</sup> Department of Life Science and Biotechnology, Jadavpur University  
Kolkata-700032, India

<sup>d</sup> Division of Molecular Medicine and Centre for Translational Research,  
Bose Institute, Kolkata-700056, India

Address for Correspondence: Papiya Nandy, [pnandy00@gmail.com](mailto:pnandy00@gmail.com)

## Graphical Abstract



## Abstract

The silver nanoparticles have found prominence in different fields such as medicine, catalysis, nanoelectronics, textile field, pollution and water treatment due to their unique attributes. Applications of silver nanoparticles are increasing rapidly in the medical purpose including drug delivery, treatment, diagnosis, medical device coating. Various chemical and physical methods are used to synthesize the silver nanoparticles (AgNP) conventionally. But these synthesis processes are expensive and also involve side effects. To solve these problems by modification in the synthesis process for safer and more efficiency, Green Nanotechnology comes to play a very crucial role for the synthesis of

*silver nanoparticles. Synthesis of biogenic silver nanoparticles from plant extract is referred as Green Nanotechnology. In this study, we have mentioned the green synthesis of silver nanoparticles using by Ocimum sanctum (Tulsi) leaf extract, which act as reducing agent as well as capping agent. Synthesized Ag nanoparticles were thoroughly characterized and their antibacterial and anticancer activities were observed. The development of brown color by the addition of Ocimum sanctum (Tulsi) signifies the formation of silver nanoparticles. UV-Vis absorption spectroscopy, XRD and zeta potential were applied to estimate the quantitative formation of silver nanoparticles. FTIR analysis was applied to reveal that the AgNPs were stabilized by eugenols, terpenes, and other aromatic compounds present in the extract. The antimicrobial and anticancer properties of AgNPs were assessed by various in vitro cellular assays. Our present study confirms that AgNP can be used as a dual therapeutic option for combating pathogenic microbial strains and hepatocellular cancer.*

## Introduction

Nanotechnology is the field for development of more consistent process for the synthesis of nanomaterials more than a range of size (with good monodispersity) and chemical composition [1]. Metallic nanoparticles have been gaining a lot of significance in the past few years due to their applicability in the field of physics, chemistry, medicine, biology and material science [2]. Metallic nanoparticles due to their high specific surface area and surface atoms have outstanding physicochemical characteristics, including optical, catalytic, electronic, magnetic and antibacterial properties. Synthesized metallic nanoparticles are enormous due to their influential applicability in various fields such as electronics, chemistry, energy, and medicine development [3]. Metallic nanoparticles, particularly noble metals are influential mainly because of their dominant optical absorption in the visible region caused by the exciting group of the free electron gas [4]. The silver nanoparticles have a wide range of interest as they have a larger number of apposite: nonlinear optics, spectrally selective coating for solar energy absorption, good electrical conductors, bio-labeling, antibacterial materials, intercalation materials for electrical batteries as optical receptors, chemically stable materials and catalyst in chemical reactions [5, 6] In the medical field, silver and silver nanoparticles have broad applications, especially in skin ointments and creams to avoid infection of burns and open wounds [10]. Silver possess an inhibitory action toward many bacterial strains and microorganisms commonly present in medical and industrial processes [7]. The general method of synthesizing silver nanoparticles in chemical reduction is as colloidal dispersions in water or organic solvents [8]. The green synthesis method is an imperative

technique, utilizes nontoxic chemicals, eco-friendly solvent and renewable materials [9] and has capability to reduce metal by specific metabolic pathway. Many biological approaches of green synthesis have been reported till date using plant leaf extracts from different plants [9, 10, 11]. These biosynthesized nanoparticles act as an antibacterial agent [12-18].

From ancient time leaves of *Ocimum sanctum* (Tulsi) is used as a remedy to cure stomachache, headache, diarrhea, dysentery, cough and cold, intestinal infections, etc. [19-24]. The leaves of the plant is aromatic, cooling, mucilaginous, diuretic and anti-inflammatory and used to treat digestive, carminative, spasmodic affections, vitiated conditions of inflammations well as a anticancer agent [25, 26, 27]. The major phytochemicals eugenol,  $\beta$ -caryophyllene,  $\beta$ -elemene, cyclopropylidene, carvacrol, linalool, germacrene, etc. present in *O. sanctum* plant are supposed to be responsible for bioreduction of silver metal ions followed by stabilization of the nanoparticles formed.

Here we have observed the effect of these biogenic AgNPs on the prokaryotic and eukaryotic cell. The phytofabricated AgNPs had a positive effect against Gram-positive (*S. aureus*, *B. subtilis*) and Gram-negative (*E. coli*, *P. aeruginosa*) pathogenic bacterial species. We have also studied the mechanism behind the bacterial growth inhibition. Our present experiments with biogenic AgNP, destruction of bacterial cell wall might have caused due to one or multiple steps of signaling cascades resulting in defective cell wall synthesis or impaired cross-linking of polymer units, which have occurred due to the ROS generation in both Gram-positive and Gram-negative bacterial strains [28, 29].

Silver ions have a great impact on altered cellular metabolism inhibiting proliferation and metastasis of cancer cells. Reactive oxygen species (ROS) generation plays a crucial role in the maintenance of the redox balance in most cancer cells and an elevated ROS level may promote oxidative damage leading to cellular abnormalities or death [30, 31]. In this study, we investigated (AgNPs) and their antimicrobial as well as anticancer activities against different pathogenic bacterial strains and hepatocellular cancer cell lines. Thus, the development of these phytofabricated, non hazardous, eco-friendly AgNPs has the potential to emerge as an effective dual therapeutic agent.

## Materials and Methods

### 1. Materials

AR-grade silver nitrate ( $\text{AgNO}_3$ ) was purchased from Sigma-Aldrich Chemicals and fresh *Ocimum sanctum* leaves were collected from local area Kolkata, India. All the chemicals and reagents required for bacterial culture media, MTT reagent, glutaraldehyde, fluorescence stains, different chemicals and reagents used for biological purposes were purchased from Merck Ltd, and SRL Pvt. Ltd, Mumbai, India at the highest grade available. All the reagents were used without further purification. Deionised (Millipore) water was used throughout the experiment with resistivity at least 18 M $\Omega$ -cm. All the glass-wares used in our experiments were cleaned with aqua regia solution followed by rinsing with ultrapure water.

#### *Bacterial strain and Cell line*

Gram-positive (*Staphylococcus aureus* 740 and *Bacillus subtilis* 441) and Gram-negative (*Escherichia coli* 443 and *Pseudomonas aeruginosa* 1688) used for the bacterial experiment were procured from Microbial Type Culture Collection (MTCC), IMTECH, Chandigarh, India.

Hep G2 are used for determine the cytotoxicity assay was obtained from Central Cell repository of National Center for Cell Science (NCCS), Pune, India.

### 2. Methods

#### *Preparation of plant leaf extract*

The leaves of *Ocimum sanctum* were washed by diionized water to remove the dust and dirt particles. The leaves are then dried at room temperature. About 2 grams of the dried powder leaves was taken in to the 100 ml distilled water. The leaves were boiled for 5 minutes and then it was allowed to cool. The solution was filtered and then stored at 4° C. All synthesis was performed within a week after preparation of leaf extract.

### ***Preparation of Silver Nitrate Solution***

1.0 mM AgNO<sub>3</sub> added in to distilled water and stirred continuously at 2 to 4 hours.

### ***Synthesis of Silver Nanoparticles***

150 ml of prepared silver nitrate stock solution was taken in a 250 ml beaker. After that, 10ml of leaf extract was added. At 90°C the mixture was heated in a water bath for 1hr.

### ***Purification of Synthesized Particles***

After heating, precipitation was obtained by centrifugation at 9000 rpm for 25 minutes. Then the precipitation was washed by centrifuged repeatedly (3 times). Thus purified Ag Nps was obtained.

### ***Physical Characterisation of Silver Nanoparticle***

The absorbance spectra were measured using Ultraviolet-visible spectrophotometer (Bio-tek) at a wavelength of 250-800 nm. Silver nano particles were synthesized by reducing silver metal ions solution with Tulsi leaf extract were initially characterized using UV-Visible Spectrophotometer. The XRD (X Ray Diffractometer) patterns of the silvernano particle samples were recorded by X-ray powder Diffractometer model D8, Bruker AXS, Winconsin, USA, using Cu-K $\alpha$  target employing wavelength of 1.5418 Å and operating at 35 kV with scan speed of 2s/step. Particle size and its distribution were assessed with field emission Scanning Electron Microscope (FESEM) using ZEISS. Electron interacts with the electrons in the sample, producing various signals that can be detected and that contain information about surface topography and composition of the samples. The Fourier transform infrared spectroscopy (FTIR) study was done using FTIR-8400S, Shimadzu in the wavenumber range from 400 cm<sup>-1</sup> to 4000 cm<sup>-1</sup>. FTIR Spectrometer to detect the possible functional groups in biomolecules present in the plant extract. The particle size distribution and stability were measured by DLS (Dynamic light Scattering) using Zetasizer (NANO ZS90, Malvern Instruments Ltd., UK). The surface charges of the nanoparticles were also measured by the Zetasizer.

### ***Antibacterial activity determination***

#### **(a) Determination of minimum inhibitory concentration (MIC) and minimum bactericidal concentration (MBC)**

According to our previously reported protocol [28, 29], MIC and MBC were evaluated by microdilution method in Luria broth. Different concentrations of AgNPs were added to the bacterial media containing the inoculums and incubated for 24 hrs. After incubation, the MIC values were obtained by checking the turbidity of the bacterial growth with UV absorption. The MBC values were determined by spreading the MIC dilutions of growth i.e. 10 µl of bacterial strain containing 2.5 × 10<sup>5</sup> CFU ml<sup>-1</sup> bacteria were separately added to the several 1 ml nutrient broths (NBs) onto agar plates and incubating them for 24 hrs at 37° C. The lowest concentration of AgNPs, at which the bacterial strains were completely inhibited, was noted as the MBC value. This MBC value of the particles denotes the minimum

concentration of particles required for 100% bacterial killing compared to the positive control (no treatment). All assays were performed in a laminar air flow.

#### (b) Tolerance level

The tolerance levels of each bacterial strain against AgNP were determined by using the following formula [28, 30].

$$\text{Tolerance} = (\text{MBC}) / (\text{MIC}) \dots\dots\dots (1)$$

#### (c) Agar well diffusion method

The susceptibility of pathogenic bacteria to AgNP was examined according to a previously reported protocol by the Agar well diffusion method. The pathogenic strains were grown on LB Broth at 37°C overnight till a turbidity of 0.5 Mac Farland standards ( $10^8$  CFU per ml). About 50µl of this suspension was used to inoculate 90mm diameter petridish filled with 30ml of Mueller Hinton Agar. Wells (diameter<sup>2</sup> = 0.563cm<sup>2</sup>) were punched in the agar plates and treated with AgNPs at their MBC concentrations. The zone of inhibition diameter in the bacterial growth surrounding the disc (including the disc) was measured [28, 30].

#### (d) Bacterial cell-viability assay

The viability of bacterial cells was analysed with help of 3-(4, 5-dimethylthiazol-2-yl) -2, 5-diphenyltetrazolium bromide (MTT) following a standard protocol [28]. Cell viability was determined after exposure to different concentrations of AgNPs for 24 hrs at 37° C. After incubation, the bacterial cells were collected and centrifuged at 1400 rpm for 10 mins at 4° C then washed three times with sterile phosphate buffered saline (PBS, pH 7.4). Subsequently, the medium was replaced with fresh culture media containing 0.5 mg.ml<sup>-1</sup> of MTT reagent and incubated for 3 hrs at 37° C. Then, HCl-isopropanol solution was added and after 15 mins of incubation at room temperature, absorbance of solubilized MTT formazan product was measured spectrophotometrically at 570 nm in a Shimadzu UV–Vis 1800 spectrophotometer.

#### (e) ROS generation in Bacterial cell

The bacterial intracellular ROS generation was measured by using 2, 7-dichlorofluorescein diacetate (DCFH<sub>2</sub>-DA) according to our previously reported protocol [29]. The DCFH<sub>2</sub>-DA passively enters the cells, reacts with the generated ROS and oxidizes as well as forming a highly fluorescent compound: 2, 7-dichlorofluorescein (DCF). After the exposure of bacteria cells with AgNPs, they were then cultured overnight and washed with PBS solutions. Then, the cells were incubated with the required amount of DCFH<sub>2</sub>-DA at 37° C for 30 mins. Finally, the bacteria cells were visualized under fluorescence microscope.

### *Anticancer Activity Determination*

#### (a) Cytotoxicity assay

The viability of Hep G2 cells after exposure to various concentrations of AgNP was determined by 3-(4, 5-dimethylthiazol-2-yl)-2,5-diphenyltetrazolium bromide (MTT) assay [31, 32, 33]. Briefly, around  $1 \times 10^4$  cells per well of 96-well plates were exposed to AgNPs at the concentrations of untreated as control, 20, 40, 60, 80, 100 µg/ml for 24 hrs of incubation at 37° C and 5% CO<sub>2</sub>. Following this, the cells were incubated again with 10 µl MTT solution (stock 1 mg/ml) for 4 h at 37°C and 5% CO<sub>2</sub> following a wash with 1× phosphate-buffered saline (PBS), and the resulting formazan crystals were dissolved in

MTT solubilization buffer to measure the absorbance at 570 nm by using a microplate reader (Biorad). The data were formulated comparing with the control ones.

**(b) Intracellular ROS generations were checked by DCFDA method in Hep G2 cells**

Normally, the DCFDA enters the cell and reacts with the reactive oxygen to give a green fluorescent color compound dichlorofluorescein (DCF). Briefly, a stock solution of DCFDA (10mM) was prepared in methanol and was further diluted with PBS to a working concentration of 100 $\mu$ M. Hep G2 cells were treated with AgNP at LD<sub>50</sub> for 12hrs at 37°C, and washed with ice-cold 1 $\times$  PBS followed by an incubation with 100 $\mu$ M of DCFDA for 30mins in the dark at 37°C [32, 33]. The fluorescence intensity was measured both spectroscopically (Hitachi, Japan) and under a fluorescence microscope in Hep G2 cells (Leica, Japan) at excitation and emission wavelengths of 485 nm and 520 nm respectively.

## Results and Discussion

### *X-ray diffraction (XRD)*

The crystalline character of these synthesized nanoparticles was confirmed by X-ray crystallography. The XRD pattern of AgNPs is given in Fig 1a. The pattern clearly shows the main peaks at (2 $\theta$ ) 38.19 and 44.37 corresponding to the (111) and (200) planes, respectively. By comparing with JCPDS (file no: 89-3722), the typical pattern of green-synthesized AgNPs is found to possess a prominent structure. The average crystalline size of the silver nanoparticles was estimated using (Eq. 2), the Debye–Scherrer’s equation

$$D=0.9\lambda/\beta \cos\theta \dots\dots\dots (2)$$

By calculating the width of (111) Bragg’s reflection, we evaluate average size of the particle is 14 nm. In addition, three unassigned peaks appeared at 27.78°, 32.34° and 46.29°. These peaks were weaker than those of silver. This may be due to the bioorganic compounds occurring on the surface of the AgNPs.

### *Fourier Transform Infrared Spectroscopy (FTIR)*

FTIR experiment was carried out in order to identify the presence of various functional groups in biomolecules responsible for the bioreduction of Ag and capping/stabilization silver nanoparticles. The obtained intense bands were compared with standard values to identify the functional groups as in Figure 2b. The bands at 3422 cm<sup>-1</sup> in the spectra corresponds to O–H stretching vibration indicating the presence of alcohol and phenol group. Bands at 2921 cm<sup>-1</sup> region arising from C–H stretching of aromatic compound were observed. The band at 1631 cm<sup>-1</sup> assigned to C–N and C–C stretching indicating the presence of proteins. The band at 1450 cm<sup>-1</sup> was assigned for N–H stretch vibration present in the amide linkages of the proteins. These functional groups have role in stability/capping of AgNP as reported in other studies. The bands at 1450 cm<sup>-1</sup> were corresponds to N–H and C–N (amines) stretch vibration of the proteins respectively. The band at 1377 cm<sup>-1</sup> exemplifies the N- O symmetry stretching typical of the nitro group.

The strong bands at 1074 cm<sup>-1</sup> are corresponds to ether linkages and suggest the presence of flavanones adsorbed on the surface of synthesized metal nanoparticles. The immediate reduction and capping of silver ion into silver nanoparticles in this analysis might be due to flavanoids and proteins. The flavonoids present in the leaf extract are powerful reducing agents which may be actively involved and responsible for the reduction of Ag<sup>+</sup> to Ag<sup>0</sup>.

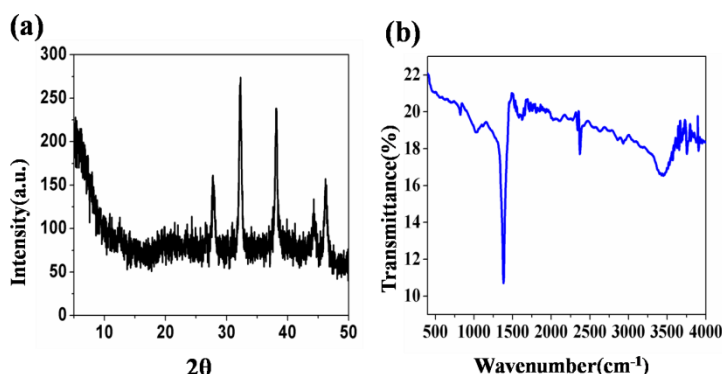


Figure.1.(a) XRD analysis of silver nanoparticles and (b) FTIR spectra

### *UV-Visible absorption studies*

The synthesized AgNPs in aqueous solution was monitored to obtain the absorption spectra at a wavelength range of 250-800 nm as shown in Figure.2a. It was observed that solution of silver nitrate turned dark brown on addition of leaves extract; it indicated the formation of AgNPs, while no color change was observed in the absence of plant extract. In the UV Vis spectrum; a single, strong and broad Surface plasmon resonance (SPR) peak was observed at 450 nm that assign the synthesis of AgNPs. Particle size distribution and surface charge measurement

### *Size Determination of Silver Nanoparticle*

Size distribution of the AgNPs was determined by DLS (Figure.2b). Particle size distribution curve reveals that AgNPs obtained are polydispersed in nature having a P.D.I (Polydispersive Index) of 0.231 with average diameter ~100 nm. The low P.D.I value indicates that the solution is homogenous in nature which is ideal for biological applications. The silver nanoparticles had quite high negative zeta potential which indicates the stability of the particles in aqueous solution. The details are given in the table below.

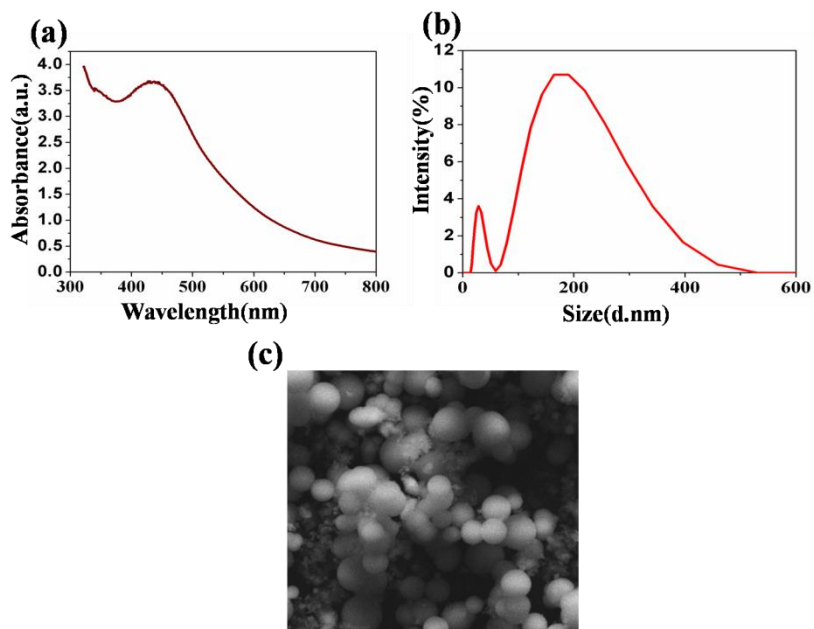


Figure.2. (a) UV-Vis spectra, (b) hydrodynamic size distribution study by DLS and (c) FESEM analysis of silver nanoparticles.

SAMPLE NAME	DLS SIZE (d.nm)	PDI	ZETA POTENTIAL (mV)
AgNP	101.8	0.231	-21.4

Table.1. Hydrodynamic Size Distribution

**Field Emission Scanning Electron Microscope (FESEM) analysis**

The FESEM images of the silver nanoparticles are shown in Figure.2c. The surface morphology of silver nanoparticles showed rod AgNP structure. In the present study, the particle size ranges from 25 to 100 nm.

**Biosynthesized AgNP nanoparticles exhibits significant antibacterial activity against pathogenic bacterial strains**

**(a) Determination of minimum inhibitory concentration (MIC) and minimum bactericidal concentration (MBC)**

To evaluate the bactericidal activity of the synthesized AgNPs have been treated separately against Gram negative *E.coli*, *P.aeruginosa* and Gram positive *S.aureus*, *B.subtilis*. In the case of *E.coli*, *P.aeruginosa* strains the MIC values of AgNP was  $38.46 \pm 1.2 \mu\text{g/ml}$ ,  $44.65 \pm 2.2 \mu\text{g/ml}$  and that in case of *S.aureus*,

*B. subtilis* the MIC value was  $35.54 \pm 1.43 \mu\text{g/ml}$ ,  $41.3 \pm 2.83 \mu\text{g/ml}$  respectively as shown in Figure.3. All bacterial strains were grown with the MIC dilutions on the sterile agar plates to obtain the MBC [28, 29]. The MBC concentrations are noted where complete bacteria growth was inhibited on the agar plate after treatment with AgNPs. The MBC values of AgNP were at  $135 \pm 3.2 \mu\text{g/ml}$ ,  $143 \pm 4.2 \mu\text{g/ml}$ ,  $132 \pm 1.8 \mu\text{g/ml}$ ,  $140 \pm 3.7 \mu\text{g/ml}$  in case of *E. coli*, *P. aeruginosa*, *S. aureus*, *B. subtilis* bacterial strains respectively. Bacterial growth decreases with an increase in the concentration of AgNP. In the microdilution method, these may be inhibited due to the easy penetration of AgNP into the cells followed by bacteriostatic in different bacterial strains.

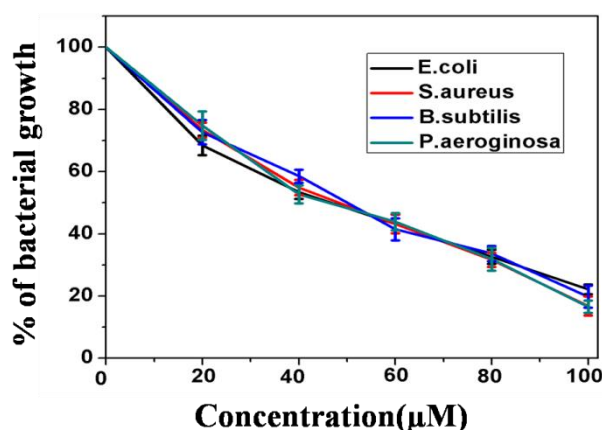


Figure.3. Analysis of activity of AgNPs by MIC method in pathogenic strains

(b) *Phytofabricated AgNPs show excellent bactericidal activity*

The tolerance level of pathogenic strains against AgNP was evaluated from the respective MIC and MBC values. From these result, it is measured that the tolerance level to AgNP was 3.5, 3.2 in case of *E. coli*, *P. aeruginosa* and 3.7, 3.4 in case of *S. aureus*, *B. subtilis* respectively. The implication of the tolerance level is the difference between bactericidal agents from bacteriostatic agents. Bactericidal agents always kill microbes, but bacteriostatic agents inhibit the growth. When the MBC/MIC ratio is greater than or equal to 16 for particular bacteria, the antibacterial agents are considered as bacteriostatic type and when this ratio is less than or equal to 4, then the particles are considered as a bactericidal agent [28]. Thus, the MBC/MIC ratio is an important parameter which reflects the bactericidal capacity of the AgNP. In this study, AgNP exhibits significant bactericidal activity against *E. coli*, *S. aureus*, *P. aeruginosa*, *B. subtilis* pathogenic strains.

(c) *Selective bactericidal activity of AgNP confirmed by Disc diffusion method*

This experiment was performed to observe the comparison of antibacterial activity of different AgNP samples. The zone of inhibitions of Gram-positive and Gram negative are given in Figure 4. Zone of inhibition having a diameter is significant when strain is treated with AgNP at their MBC concentration. So, from this study, it has become clear that the AgNP has really proved to be beneficial and needs to be administered for pathogenic *E. coli*, *S. aureus*, *B. subtilis*, *P. aeruginosa* growth inhibition.

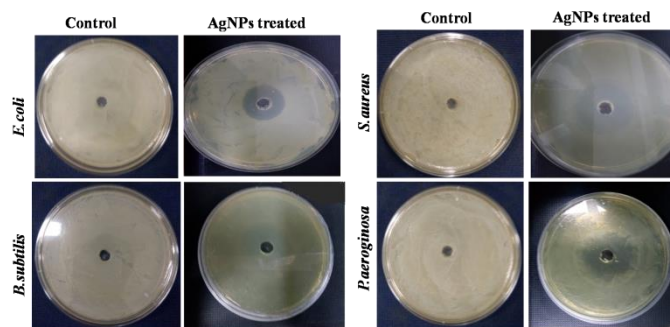


Figure.4. Antibacterial assessment of biogenic silver nanoparticles in pathogenic strains by disc agar diffusion method.

(d) **Treatment of *E.coli*, *S.aureus*, *B.subtilis*, *P.aeruginosa* with AgNP significantly diminishes the bacterial cell viability**

AgNP is responsible for diminishing the bacterial cell survivability at their respective MBC conc. as depicted in Figure.5. This may be due to the ingress of AgNPs into the bacterial cells that can hinder the growth of the bacteria and acts as an ideal bactericidal agent.

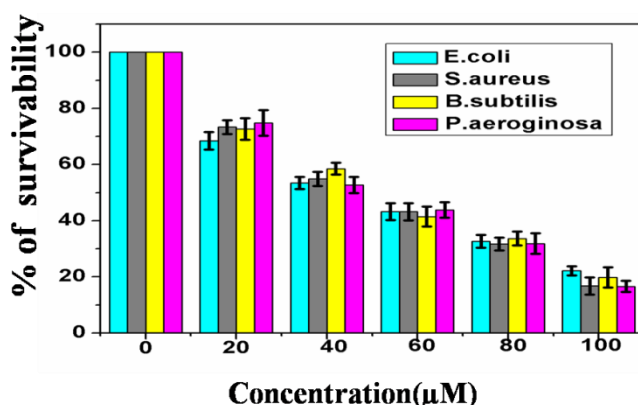
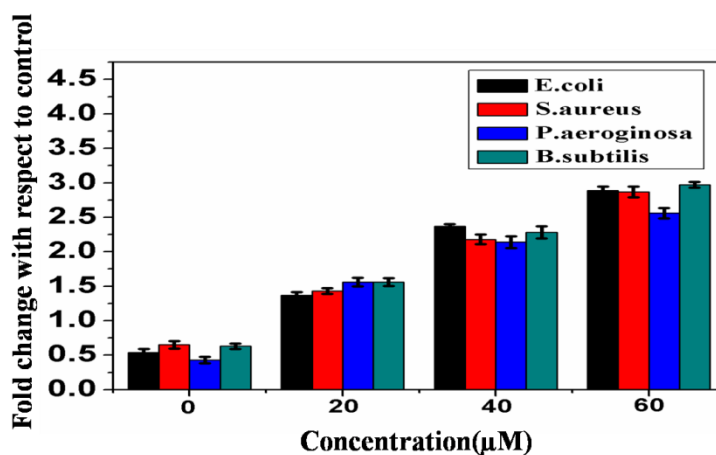


Figure.5. Bacterial viability study upon treatment with AgNPs in pathogenic bacterial strains

(e) **Mechanisms behind bactericidal activity of functionalized AgNPs**

The phytofabricated AgNPs had the capability to induce intracellular ROS generation which in turn culminates in the bacterial cell death. In order to envisage the mechanisms behind the bactericidal activities of AgNPs, the intracellular ROS generation in the bacterial cells was determined by employing DCFH-DA as an intracellular ROS indicator which is depicted in Figure.6. The results indicate that the AgNP treated pathogenic bacterial cells augment the generation of ROS which is responsible for bacterial cell death. The enhanced ROS production is correlated with bacterial cell death. The intracellular ROS production contributes to the bacterial cell membrane damage, disruption in the electronic transport chain and the genetic material detonation [29, 30].



**Figure.6. Intracellular ROS generation by treatment with AgNPs in pathogenic bacterial strains.**

### *Anticancer activity of AgNPs*

#### *(a) Cytotoxicity of AgNPs*

The in vitro cytotoxicity of the AgNPs is evaluated for determining the cytotoxic effects on HepG2 cell line. The cells were exposed to different concentrations of AgNPs (0-120 µg/ml) for a time span of 24hrs and was afterwards followed by MTT assay. It was observed that the AgNPs depicted a dose dependent decrease in the cell survivability. The LD<sub>50</sub> of AgNP was calculated to be  $46 \pm 3.2$  µM. Thus we can conclude that the synthesized phytofabricated AgNPs could exert encouraging anticancer activity as exhibited in Figure.7.

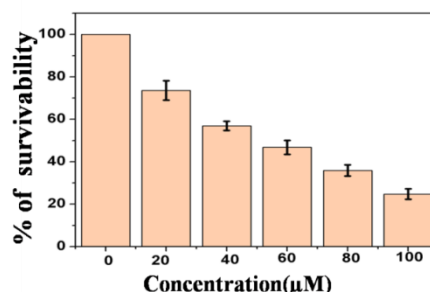


**Figure.7. Cell viability assay of HAP in human hepatocellular carcinoma, HepG2**

#### *(b) Intracellular Reactive oxygen species generation induced by treatment of AgNP*

The Reactive oxygen species (ROS) is analysed with the the dual aid of fluorescence microscopy and Spectro fluorometer by employing 2', 7' dichlorofluoresce in diacetate (DCF-DA) as a probe. The generation of reactive oxygen species is evaluated in case of hepatocellular carcinoma cells, Hep G2 with AgNPs at concentrations of 80 µM and 100 µM for 12hrs. The fluorescence microscopic images

clearly depicts that the enhancement of green color fluorescent intensity occurred in case of treated HepG2 cell lines after 12hrs ( Figure. 8a and 8b).

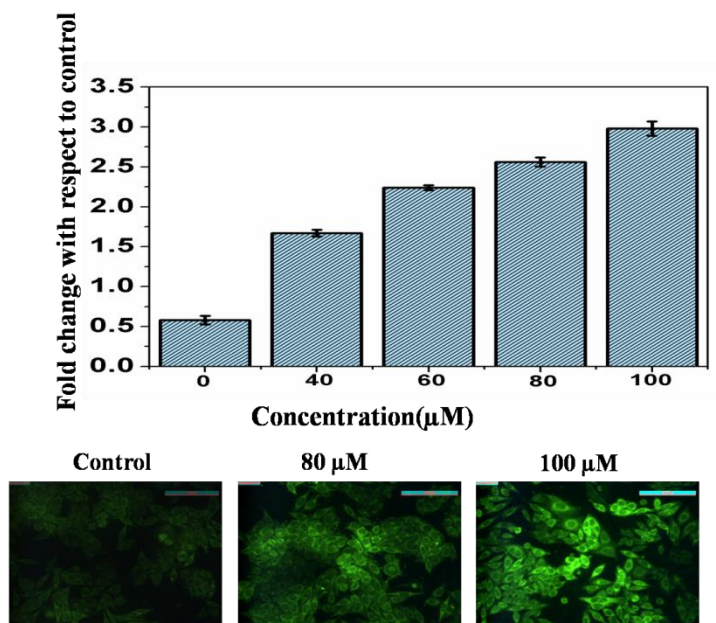


**Figure.8. Intracellular ROS generation by treatment with AgNPs in HepG2 cells observed by (a) spectrofluometry and (b) fluorescence microscopy**

## Conclusions

The synthesis of phytofabricated silver nanoparticle is inexpensive, non toxic and ecofriendly. The AgNPs were thoroughly charecterised with the UV-Vis, FTIR, XRD, DLS and FESEM. The results from UV-Vis spectral studies testified the presence of surface plasmon resonance of these biogenic silver nanoparticles. The biomolecules predominant in the *O. sanctum* leaves were primarily responsible for reducing and capping of AgNPs which were then analysed by FTIR measurements. Particle size and stabilization were determined with the aid of DLS and zeta potential techniques. FESEM studies depicted the formation of rod and uniform shaped silver nanoparticles with a size range of 25-100 nm. The XRD pattern additionally confirmed the development of the silver nanoparticles via the eco-friendly green synthetic route.

Although there has been significant progress in cancer diagnosis and treatment, cancer is still posing a worldwide grave threat. On the other hand, the global dissemination of pathogenic bacterial strains has emerged as a serious cotemporary challenges with respect to public health. Our results clearly depicts that the biogenic AgNPs are responsible for initiating the oxidative damage through augmented ROS generations both in case of prokaryotic and eukaryotic cells. The generated reactive oxygen or superoxide has the potential to directly interact with the cell metabolism in order to generate the hydroxyl radicals, which is responsible for damaging the DNA, lipid and proteins. Our results clearly suggest that these phytofabricated AgNPs can be considered as potential antibacterial agent against Gram-positive (*S. aureus*, *B. subtilis*) and Gram-negative (*E. coli*, *P. aeruginosa*) pathogenic bacterial strains.

In the present study with AgNPs, the probable reason behind the bacterial cell wall destruction might be the disruption in the steps of signaling cascades that leads to the defective cell wall synthesis. This phenomenon takes place due to the enhanced ROS generation in both Gram-positive and Gram-negative bacterial strains. Additionally, the phytofabricated leads to the death of human liver cancer due to enhanced intracellular ROS. In conclusion, our studies suggest that our phytofabricated AgNPs can emerge as potential anticancer and antibacterial agents.

## References

1. M. Rai, A. Gade, A. Yadav, Biogenic nanoparticles: an introduction to what they are, how they are synthesized and their applications. In: Rai M, Duran N (eds), *Metal nanoparticles in microbiology* pp 1–16 (2011).
2. K. Yokohama, D.R. Welchons The conjugation of amyloid beta protein on the gold colloidal nanoparticles surfaces, *Nanotechnology* **18**:105101–105107 (2007).
3. A. Saxena, R.M. Tripathi, F. Zafar, P. Singh, Green synthesis of silver Nanoparticles using aqueous solution of *Ficus benghalensis* leaf extract and characterization of their antibacterial activity, *Mater Lett.* **67** 91–94 (2012).
4. M.B. Mohamed, V. Volkov, S. Link, M.A.E. Sayed, The ‘lightning’ gold nanorods: fluorescence enhancement of over a million compared to the gold metal, *Chem Phy Lett.* **317** 517–523 (2000).
5. M. Zargar, S. Shameli, N. G. Reza, F. Farahani, Plant mediated green biosynthesis of silver nanoparticles using *Vitex negundo* L. extract. *J Ind Eng Chem.* **20(6)** 4169–4175 (2014).
6. H. Jiang, S. Manolache, A.C.L. Wong, F.S. Denes, Plasma enhanced deposition of silver nanoparticles onto polymer and metal surfaces for the generation of antimicrobial characteristics, *J Appl Polym Sci.* **93** 1411–1422 (2004).
7. V.K. Sharma, R.A. Yngard, Y. Liny, Silver nanoparticles; green synthesis and their antimicrobial activities, *Adv Coll Interface Sci.* **145** 83–96 (2009).
8. P. Raveendran, J. Fu, S.L. Wallen, Completely green synthesis and stabilization of metal nanoparticles *J Am Chem Soc.* **125** 13940–13941(2003).
9. S.A. kumar, S. Ravi, V. Kathiravan, S. Velmurugan, Synthesis, characterization and catalytic activity of silver nanoparticles using *Tribulus terrestris* leaf extract, *Spectrochimica Acta Part A: Molecular and Biomolecular Spectroscopy* **121** 88-93 (2014).
10. S.P. Chandran, M. Chaudhary, R. Pasricha, A. Ahmed, M. Sastry, Synthesis of gold nanotriangles and silver nanoparticles using *Aloe vera* plant extract, *Biotechnology Progress,* **22** 577-583 (2006).
11. S.P. Dubey, M. Lahtinen, M. Sillanpaa, Tansy fruit mediated greener synthesis of silver and gold nanoparticles, *Process Biochemistry* **45** 1065-1071(2010).
12. R.N. Rati, P. Nilotpala, B. Debadhyan, M.P. Kshyama, M. Srabani, B.S. Lala, B.K. Mishra, Green synthesis of silver nanoparticle by *Penicillium purpurogenum* NPMF: the process and Optimization, *Journal of Nanoparticles Research* **13** 3129-3137 (2011).
13. N. Duran, P.D. Marcato, G.I.H. DeSouza, O.L. Alves, E. Esposito, Antibacterial effect of silver nanoparticles produced by fungal process on textile fabrics and their effluent treatment, *Journal of biomedical nanotechnology* **3** 203-208 (2007).
14. S. Edgar, S. Sofia, M. Sonia, J. Correia, PVP coated silver nanoparticles showing antifungal improved activity against Dermatophytes, *Journal of nanoparticles research* **16** 2726 (2014).
15. A.M. Fayaz, K. Balaji, M. Girilal, R. Yadav, P.T. Kalaichelvan, R. Venketesan, Biogenic synthesis of silver nanoparticles and their synergistic effect with antibiotics: a study against gram-positive and gram-negative bacteria, *Nanomedicine: Nanotechnology, Biology and medicine* **6** 103-109 (2010).
16. Q.L. Feng, J. Wu, G.Q. Chen, F.Z. Cui, T.N. Kim, J.O. Kim, A mechanistic study of the antibacterial effect of silver ions on *Escherichia coli* and *Staphylococcus aureus*, *Journal of Biomedical Materials Research* **52** 662-668 (2001).
17. S. Ghosh, S. Patil, M. Ahire, R. Kitture, S. Kale, K. Pardesi, S.S. Cameotra, J. Bellare, D.D. Dhavale, A. Jabgunde, B.A. Chopade, Synthesis of silver nanoparticles using *Dioscorea bulbifera* tuber extract and evaluation of its synergistic potential in combination with antimicrobial agents, *International journal of Nanomedicine* **7** 483-496 (2012).
18. S. Kaviya, J. Santhanalakshmi, B. Viswanathan, J. Muthumar, K. Srinivasan, Biosynthesis of silver nanoparticles using citrus sinensis peel extract and its antibacterial activity, *Spectrochimica Acta Part A: Molecular and Biomolecular Spectroscopy,* **79** 594-598 (2011).
19. N. Singh, Y. Hoette, R. Miller, Tulsi: The Mother Medicine of Nature. 2nd ed. Lucknow: *International Institute of Herbal Medicine* pp. 28–47 (2010).
20. N. Mahajan, S. Rawal, M. Verma, M. Poddar, S. Alok, A phytopharmacological overview on *Ocimum* species with special emphasis on *Ocimum sanctum*, *Biomed Prev Nutr.* **3** 185–92 (2013).

21. L. Mohan, M.V. Amberkar, M. Kumari, *Ocimum sanctum* linn. (TULSI)- an overview, *Int J Pharm Sci Rev Res.* **7** 51-3(2011).
22. P. Pattanayak, P. Behera, D. Das, S.K. Panda, *Ocimum sanctum* Linn. A reservoir plant for therapeutic applications: An overview, *Pharmacogn Rev.* **4** 95–105 (2010).
23. M.M. Cohen, Tulsi - *Ocimum sanctum*: A herb for all reasons, *J Ayurveda Integr Med.* **5(4)** 251–259 (2014).
24. S. Mondal, B.R. Mirdha, S.C. Mahapatra, The science behind sacredness of Tulsi (*Ocimum sanctum* Linn.) *Indian J Physiol Pharmacol.* **53** 291–306 (2009).
25. W. Wangcharoen, W. Morasuk, Antioxidant capacity and phenolic content of holy basil Songklanakarin, *J Sci Technol.* **29** 1407–15 (2007).
26. V.S. Panda, S.R. Naik, Evaluation of cardioprotective activity of Ginkgo biloba and *Ocimum sanctum* in rodents, *Altern Med Rev.* **14** 161–71 (2009).
27. M. Shivananjappa, M. Joshi, Aqueous extract of *tulsi* (*Ocimum sanctum*) enhances endogenous antioxidant defenses of human hepatoma cell line (HepG2) *J Herbs Spices Med Plants* **18** 331–48 (2012).
28. Bera D, Pal K, Bardhan S, Roy S, Parvin R, Karmakar P, Nandy P, Das Sukhen 2019 Functionalised biomimetic hydroxylapatite NPs as potential agent against pathogenic multidrug- resistant bacteria *Advances in Natural Sciences: Nanoscience and Nanotechnology* **10** 045017
29. S. Bardhan, K. Pal, S. Roy, S. Das, A. Chakraborty, P. Karmakar, R. Basu, S. Das, Nanoparticle size-dependent antibacterial activities in natural minerals, *Journal of Nanoscience and Nanotechnology* doi: 10.1166/jnn.2019.16658
30. S.P. Chakraborty, S.K. Sahu, S.K. Mahapatra, S. Santra, M. Bal, S. Roy, P. Pramanik, Nanoconjugated vancomycin: new opportunities for the development of anti-VRSA agents, *Nanotechnology* **21** 105103–11 (2010).
31. J. Mandal, P. Ghorai, K. Pal, P. Karmakar, A. Saha, 2-hydroxy-5-methylisophthalaldehyde based fluorescent-colorimetric chemsensor for dual detection of Zn Cu<sup>2+</sup> with high sensitivity and application in live cell imaging, *Journal of Luminescence* **205** 14–22 (2019).
32. K. Pal, S. Roy, P.K. Parida, A. Dutta, S. Bardhan, S. Das, K. Jana, P. Karmakar, Folic acid conjugated curcumin loaded biopolymeric gum acacia microsphere for triple negative breast cancer therapy in invitro and invivo model, *Materials Science & Engineering C* **95** 204-216 (2019).
33. K. Pal, D. Laha, P.K. Parida, S. Roy, S. Bardhan, A. Dutta, K. Jana, P. Karmakar, An in vivo study for targeted delivery of curcumin in Human triple negative breast carcinoma cells using biocompatible PLGA microspheres conjugated with folic acid, *Journal of Nanoscience and Nanotechnology* **19** 3720-3733 (2019).